A Novel THM Framework for Investigating Time-Dependent Behavior of Frozen Soils

Dana Amini[*,1,2], Amade Pouya[2], and Pooneh Maghoul[1,3]

[1]*Sustainable Infrastructure and Geoengineering Laboratory (SIGLab), Department of Civil Engineering, University of Manitoba, Manitoba, Canada*

[2]*Navier Laboratory, École des Ponts ParisTech, Champs-sur-Marne, France*

[3]*Sustainable Infrastructure and Geoengineering Laboratory (SIGLab), Department of Civil, Geological and Mining Engineering, Polytechnique Montréal, Montréal, Quebec, Canada*

[*]*Corresponding author's email:* aminid@myumanitoba.ca

Abstract: The performance of infrastructure in northern regions, impacted by frost action and climate change, heavily depends on the response of frozen foundations, both in the short and long term. Investigating these effects requires advanced constitutive modeling and multiphysics analyses, involving heat transfer, mass transfer, and mechanical processes. To this end, this study introduces a novel Thermo-Hydro-Mechanical (THM) formulation developed to explore the complex time- and temperature-dependent behavior of frozen soils. Contrary to conventional modeling approaches, the framework considers the medium as a deformable solid mixture of ice and soil grains, and a porous space filled with unfrozen water. This distinction marks a significant advancement in mechanical modeling, facilitated by an advanced non-isothermal strain-rate constitutive model capable of capturing time- and temperature-dependent (thermal creep) deformations. Moreover, the hydraulic governing equations are developed by deriving volumetric ice and water contents, considering their temperature-dependent reciprocal interactions over time, accounting for unfrozen water as the fluid migrating through the solid mixture. Furthermore, the thermal aspect accurately accounts for energy conservation, specifically addressing the latent heat effects resulting from phase transitions between water and ice.

Introduction

The development of infrastructure in cold regions relies heavily on the response of traditionally frozen foundations to frost action. It necessitates a thorough understanding of the complex physical processes governing ice- and water-saturated porous geomaterials under both short- and long-term thermal variations. These processes include phase transitions, multiphase interactions, water conduction and convection, and thermal effects. Addressing these phenomena requires advanced analyses that simultaneously integrate heat transfer, mass transfer, and mechanical deformation through the framework of coupled Thermo-Hydro-Mechanical (THM) modeling theory.

To develop a rigorous THM framework for frozen soils, several key complexities arising from the coexistence of ice and water must be addressed: (1) the reduced permeability caused by ice formation, which restricts unfrozen water migration; (2) latent heat effects associated with phase transitions, which alter the heat capacity of the mixture; (3) variations in thermal conductivity driven by ice content; and most critically, (4) the inherent nonlinearities in mechanical responses, which cannot be adequately described by linear constitutive laws. The mechanics of frozen soils are characterized by temperature-dependent mechanical strength and inter-particle forces arising from ice within the pore spaces. In addition, frozen soils exhibit slow, irreversible, time-dependent deformation (i.e., viscous or creep behavior) under sustained stress and temperature conditions. It necessitates the use of advanced nonlinear geomechanical constitutive models capable of accurately capturing the rate-dependent response of frozen soils, a feature that is sporadically incorporated within the existing THM frameworks.

This study presents a new THM framework designed to investigate the time- and temperature-dependent behavior of saturated frozen soils. The proposed framework distinguishes itself from existing models by (1) conceptualizing frozen soils as a porous medium consisting of a deformable solid mixture of ice and soil grains, with water-infiltrated pore spaces at any given time, reflecting a specific unfrozen water saturation, and (2) integrating a non-isothermal strain-rate constitutive model to accurately capture the complexities of thermal creep deformations. This approach offers a more comprehensive understanding of the coupled thermal, hydraulic, and mechanical processes that govern the behavior of saturated frozen soils.

Thermo-Hydro-Mechanical Framework

This section explains the mathematical equations that govern the thermo-hydro-mechanical (THM) processes. Three independent variables of volumetric strain (ε_v), pore water pressure (P_w), and temperature (T) are selected as the primary variables for the derivation of governing equations.

In general a saturated (partially) frozen soil is a continuum body composed of a deformable skeleton (i.e., soil grains) and a porous space filled with unfrozen water and ice. The volumetric fractions of soil grains, θ_s, unfrozen water, θ_w, and ice content, θ_i, can be described as follows:

$$\theta_s = 1 + \varepsilon_v - \phi, \qquad \theta_w = \phi S_w, \qquad \theta_i = \phi(1 - S_w), \qquad \phi = \theta_w + \theta_i \tag{1}$$

where $\phi = V_\phi / V_0$ is the Lagrangian porosity in which V_ϕ and V_0 are the pore volume and the initial volume of the medium, respectively; $S_w = V_w / V_\phi$ and V_w are the degree of saturation relative to water and the volume of water in voids, respectively.

As noted earlier, in the present study ice crystals are considered a part of the solid skeleton, hereinafter referred to as the solid phase. In essence, the presented framework considers the medium as a deformable porous solid mixture of ice and soil grains, with the pore spaces occupied by unfrozen water. Such consideration allows for the introduction of a new THM framework in accordance with the key principles outlined in the *Poromechanics* of saturated unfrozen porous media [1]. To this end, the saturated frozen soil in its current state, corresponding to a certain S_w, can be represented by a substitute porous medium with the Lagrangian porosity of $\phi^* = S_w \phi$. Thus, the evolution of the Lagrangian porosity of ϕ^* can take the form of

$$\delta\phi^* = -b^* \delta\varepsilon_v + \frac{1}{N_b^*} \delta P_w \tag{2}$$

Substituting $\delta\phi^*$ by $S_w \delta\phi$ gives

$$S_w \delta\phi = -b^* \delta\varepsilon_v + \frac{1}{N_b^*} \delta P_w \tag{3}$$

For the purpose of the present work, b^* and $1/N_b^*$ are respectively expressed as $S_w b$ and S_w/N_b where b is the Biot's coefficient and N_b is the Biot's modulus of the skeleton related to the Biot's modulus M_b by $1/N_b = 1/M_b - \phi/K_w$ (K_w is the compressibility of water).

Conservation of linear momentum

The equation of mechanical equilibrium (conservation of linear momentum), in the absence of inertial terms, can be expressed as follows:

$$\nabla \cdot \boldsymbol{\sigma} + \boldsymbol{B} = 0 \tag{4}$$

where $\boldsymbol{\sigma}$ $(= \sigma_{ij})$ is the total stress tensor and $\boldsymbol{B}$ $(= -\rho g_i)$ denotes the body forces vector due to gravity; and $\rho = \rho_{s_0}(1 - \phi_0) + \rho_w \theta_w + \rho_i \theta_i$ in which ρ_s, ρ_w, and ρ_i are the density of the solid skeleton, water and ice, respectively.

The development of a coupled model for frozen soils requires two constitutive laws to capture the effects of cryogenic suction on solid-phase deformation and unfrozen water saturation. The first is a stress-cryosuction-strain relationship, which accounts for the impact of cryogenic suction on mechanical strength and strain. The second is a temperature-saturation relation, linking water saturation to negative temperatures (or cryogenic suction). The thermo-elasto-viscoplastic (TEVP) model proposed by Amini et al. [2] is used for the first law, while the second is derived using a thermodynamic state function representing the unfrozen water saturation characteristic curve (UWSCC). These considerations are discussed in the following subsections.

Mechanical Constitutive Model

The TEVP constitutive model developed by Amini et al. [2] is based on the two state variables framework where the solid phase stress and cryogenic suction are the two state variables. The solid phase stress is defined by characterizing the solid phase as a combination of ice crystals and a solid skeleton and formulated as follows:

$$\boldsymbol{\sigma}^* = \boldsymbol{\sigma} - b^* P_w \boldsymbol{I} \tag{5}$$

in which $\boldsymbol{\sigma}$ $(= \sigma_{ij})$ denotes the total stress tensor; $\boldsymbol{I}$ $(= I_{ij})$ is the second-order isotropic tensor with component δ_{ij}, where δ_{ij} is the Kronecker delta, which returns values of 0 for $i \neq j$ and 1 for $i = j$. The cryogenic suction, S, as the second stress state variable is defined as:

$$S = P_i - P_w \tag{6}$$

in which P_i and P_w denote the pressure of the ice and water phases, respectively. The cryogenic suction can be approximated by the thermodynamic equilibrium at the ice-water interface described by the Clausius–Clapeyron equation as follows:

$$S \approx -\rho_w L \ln\left(T/T_{ref}\right) \tag{7}$$

where L is the latent heat of freezing due to the phase change of water (approximately 3.34×10^5 J kg^{-1}), T indicates temperature, and T_{ref} is the reference temperature (typically 273.15 K).

The TEVP constitutive model describes the stress-strain relationship in a rate form as follows:

$$\dot{\boldsymbol{\sigma}}^* = \boldsymbol{C}^e \dot{\boldsymbol{\varepsilon}}^{\sigma e} \tag{8}$$

where the over-dot indicates the time rate of change; $\boldsymbol{C}^e$ $(= C^e_{ijkl})$ is the fourth order elastic stiffness matrix; and $\dot{\boldsymbol{\varepsilon}}^{\sigma e}$ $(= \dot{\varepsilon}^{\sigma e}_{ij})$ is the second-order elastic strain rate tensor due to changes in solid phase stress, $\boldsymbol{\sigma}^*$ $(= \sigma^*_{ij})$.

The elastic stiffness tensor, $\boldsymbol{C}^e$, is populated in terms of the temperature-dependent shear modulus, G_T, and bulk modulus, K_T, of the porous solid phase (with zero pore water pressure) defined as follows:

$$G_T = S_w G_o + (1 - S_w)\frac{E_f}{2(1+\nu_f)} \tag{9}$$

$$K_T = S_w K_o + (1 - S_w)\frac{E_f}{3(1-2\nu_f)} \tag{10}$$

where G_o and K_o $(= V p^*_o/\kappa_o)$ are, respectively, the shear modulus and bulk modulus of the soil in the unfrozen state; p^*_o is the pre-consolidation stress in the unfrozen state; κ_o stands for the compressibility coefficient within the elastic region; ν_f Poisson's ratio of frozen soil; and E_f is Young's modulus of the soil in the fully frozen state empirically expressed as follows:

$$E_f = E_{ref}\Big[1 - a_E\left(T - T_{ref}\right)\Big] \tag{11}$$

where E_{ref} is Young's modulus of the frozen soil at the reference temperature; a_E is a material parameter denoting the change in E_f with temperature change.

In the TEVP model, the total strain rate, $\dot{\boldsymbol{\varepsilon}}$, consists of two mechanical (solid phase stress-dependent), $\dot{\boldsymbol{\varepsilon}}^{\sigma}$, and cryogenic suction-dependent, $\dot{\boldsymbol{\varepsilon}}^{suc}$, components. The strain rate due to changes in solid phase stress is decomposed into elastic (time-independent recoverable) and thermo-viscoplastic (time- and temperature-dependent irrecoverable) components ($\dot{\boldsymbol{\varepsilon}}^{\sigma e}$ and $\dot{\boldsymbol{\varepsilon}}^{\sigma Tvp}$). Hence

$$\dot{\boldsymbol{\varepsilon}}^{\sigma e} = \dot{\boldsymbol{\varepsilon}} - \dot{\boldsymbol{\varepsilon}}^{\sigma Tvp} - \dot{\boldsymbol{\varepsilon}}^{suc} \tag{12}$$

where the over-dot indicates the rate of change ($\dot{\varepsilon}_{ij} = \delta\dot{\varepsilon}_{ij}/\delta t$, where t is the time). The TEVP model considers strain rate due to cryogenic suction changes ($\dot{\boldsymbol{\varepsilon}}^{suc}$) to be elastic and volumetric expressed as follows:

$$\dot{\boldsymbol{\varepsilon}}^{suc} = \left(\boldsymbol{C}^{suc}\right)^{-1}\dot{S} = \left(\frac{1}{3V_0}\frac{\kappa_s}{S + P_{atm}}\boldsymbol{I}\right)\dot{S} \tag{13}$$

where $\dot{S}$ denotes the cryogenic suction rate and $\boldsymbol{C}^{suc}$ is the elastic cryogenic suction–strain tensor; κ_s is the elastic stiffness parameter for changes in cryogenic suction; and P_{atm} is the atmospheric pressure. Thermo-viscoplastic strain rates ($\dot{\boldsymbol{\varepsilon}}^{\sigma Tvp}$) at the current stress state of the soil ($\boldsymbol{\sigma}$,S) are given by

$$\dot{\boldsymbol{\varepsilon}}^{\sigma Tvp} = \underbrace{\left(\eta \frac{\psi_T}{V_m} \frac{\mathrm{Li}^{-1}(\Phi)}{\ln\left(\mathrm{Li}^{-1}(\Phi)\right)} \frac{1}{|\partial F_{VPPS}/\partial p^*|} \right)}_{\Lambda:\ \text{Scalar Multiplier}} \frac{\partial F_{VPPS}}{\partial \boldsymbol{\sigma}^*} \tag{14}$$

where V_m stands for the time-dependent specific volume of the frozen geomaterial under isotropic compression (p^*_m) corresponding to the current stress state, η is a temperature- and stress-dependent parameter controlling the creep going into the tertiary stage, ψ_T is a temperature- (or cryogenic suction-) dependent creep parameter, F_{VPPS} stands for the viscoplastic potential surface (VPPS) passing through the current stress state, p^* is the mean solid phase stress, and

$$\Phi = \frac{V_m - N_f + \lambda_f \ln p^*_m}{-\psi_T} + \mathrm{Li}\big(\exp(\eta t_o)\big) \tag{15}$$

in which λ_f is the elastoplastic compressibility coefficient of the geomaterial in a frozen state, N_f is the specific volume at unit pressure in the current cryogenic suction, t_o is a material parameter denoting the initiation time of purely creep compression deformations, and Li denotes logarithmic integral function. The readers are referred to [2] for more detailed explanation of the TEVP model.

Unfrozen Water Saturation Characteristic Curve (UWSCC)

The amount of water that remains in the unfrozen state as the soil freezes is a characteristic of the soil, and the unfrozen water saturation characteristic curve (UWSCC) is used to describe the relationship between unfrozen water saturation and freezing temperature. The Young-Laplace law describes the capillary pressure difference (P_i-P_w) across the interface between unfrozen water and ice. Given the analogy between freezing-thawing cycles in frozen soils and drying-wetting cycles in unsaturated soils, the unfrozen water saturation can be expressed as a function of capillary pressure. By substituting capillary pressure with cryogenic suction and subsequently replacing cryogenic suction with temperature, the relationship between unfrozen water saturation and temperature can be derived as follows:

$$S_w = \left(1 + \left(-\frac{\ln(T/T_{ref})}{\mu} \right)^{1/(1-m)} \right)^{-m} \tag{16}$$

Here, $\mu = N_c \gamma_{iw}/\rho_w L \gamma_{aw}$ where N_c represents the capillary modulus, γ_{iw} and γ_{aw} are the unfrozen water-ice and water-air interface energies, respectively, and m is a constant material parameters that characterizes the shape of the capillary curve.

Conservation of mass

The mass conservation equation for pore water can be written as:

$$\frac{\partial m_f}{\partial t} + \nabla \cdot (\rho_w \boldsymbol{q}^w) = r^{H_0} \tag{17}$$

where r^{H_0} is a sink/source term, $m_f = \rho_w \theta_w + \rho_i \theta_i$ is the total fluid mass per unit volume, and $\boldsymbol{q}^w$ is the water flux vector:

$$\boldsymbol{q}^w = -\frac{\boldsymbol{K}^{S_w}}{\rho_w g} \nabla(\Psi + \rho_w \boldsymbol{g} z) \tag{18}$$

where Ψ is the seepage pressure that consists of the pore water pressure (P_w) and the cryogenic suction (S)[1]; and $\boldsymbol{K}^{S_w}$ is the saturation-dependent hydraulic conductivity matrix that can be expressed as follows:

$$\boldsymbol{K}^{S_w} = \boldsymbol{K} \sqrt{S_w} \left[1 - \left(1 - S_w{}^{\frac{1}{m}} \right)^m \right]^2 \tag{19}$$

where $\boldsymbol{K}$ $(= K\delta_{ij})$ is the saturated hydraulic conductivity matrix and m is a material parameter described earlier.

Eq. 17 can take the form of

$$\frac{\partial(\rho_w \theta_w)}{\partial t} + \nabla \cdot (\rho_w \boldsymbol{q}^w) = r^{H_0} - \frac{\partial(\rho_i \theta_i)}{\partial t} \tag{20}$$

which can be rewritten by expanding the time derivatives as follows:

$$\left(\theta_w \frac{\partial \rho_w}{\partial t} + \rho_w \frac{\partial \theta_w}{\partial t} \right) + \nabla \cdot (\rho_w \boldsymbol{q}^w) = r^{H_0} - \left(\frac{\partial(\rho_i \theta_i)}{\partial \varepsilon_v} \frac{\partial \varepsilon_v}{\partial t} + \frac{\partial(\rho_i \theta_i)}{\partial P_w} \frac{\partial P_w}{\partial t} + \frac{\partial(\rho_i \theta_i)}{\partial T} \frac{\partial T}{\partial t} \right) \tag{21}$$

The mass of ice in the volume (i.e., $\rho_i \theta_i V_0$) depends only on temperature; thus, Eq. 21 can be reduced to

$$\theta_w \frac{\partial \rho_w}{\partial t} + \rho_w \frac{\partial \theta_w}{\partial t} + \nabla \cdot (\rho_w \boldsymbol{q}^w) = r^{H_0} - \left(\theta_i \frac{\partial \rho_i}{\partial T} + \rho_i \frac{\partial \theta_i}{\partial T} \right) \frac{\partial T}{\partial t} \tag{22}$$

Substituting $\partial \rho_w / \partial t = \dfrac{\rho_w}{K_w} \partial P_w / \partial t$, $\partial \rho_i / \partial T = 0$, and $\partial \theta_i / \partial T = -\phi \partial S_w / \partial T$ and recalling:

$$\frac{\partial \theta_w}{\partial t} = -b^* \frac{\partial \varepsilon_v}{\partial t} + \frac{1}{N_b^*} \frac{\partial P_w}{\partial t} + \phi \frac{\partial S_w}{\partial T} \frac{\partial T}{\partial t} \tag{23}$$

leads to the final form of the conservation of mass equation as follows:

$$\rho_w \left(\frac{\theta_w}{K_w} + \frac{1}{N_b^*} \right) \frac{\partial P_w}{\partial t} + \nabla \cdot \left(-\rho_w \frac{\boldsymbol{K}^{S_w}}{\rho_w g} \nabla(\Psi + \rho_w \boldsymbol{g} z) \right) = r^{H_0} + \rho_w b^* \frac{\partial \varepsilon_v}{\partial t} - (\rho_w - \rho_i) \phi \frac{\partial S_w}{\partial T} \frac{\partial T}{\partial t} \tag{24}$$

Conservation of energy

The energy conservation equation takes the following form:

$$\frac{\partial E}{\partial t} + \nabla \cdot \left(\boldsymbol{q}^{T_{cnd}} + \boldsymbol{q}^{T_{adv}} \right) = r^{T_0} \tag{25}$$

[1] Cryogenic suction is embedded in the seepage potential, allowing the formulation to capture freezing-induced water migration toward colder zones where ice nucleation dominates.

where $\boldsymbol{q}^{T_{cnd}}$ denotes the heat conduction flux vector defined as

$$\boldsymbol{q}^{T_{cnd}} = -\lambda_T \nabla T \tag{26}$$

in which $\lambda_T = \lambda_s(1-\phi_0) + \lambda_w\theta_w + \lambda_i\theta_i$ with λ_s, λ_w, λ_i the heat conductivity of solid skeleton, water, and ice, respectively; $\boldsymbol{q}^{T_{adv}}$ stands for the heat advected by flowing water expressed as:

$$\boldsymbol{q}^{T_{adv}} = \rho_w c_w T \boldsymbol{q}^w \tag{27}$$

with c_w specific heat capacity of water; r^{T_0} is the sink/source term of energy; and E is the volumetric internal energy of soil that can be described in incremental form as follows:

$$\delta E = C_p \delta T - L\delta(\rho_i\theta_i) \tag{28}$$

in which $C_p = c_s\rho_{s_0}(1-\phi_0) + c_w\rho_w\theta_w + c_i\rho_i\theta_i$ is the volumetric heat capacity of the mixture; c_s, c_w, c_i are specific heat capacities for the solid skeleton, water, and ice, respectively.

Eq. 25 can be slightly reformed as follows:

$$C_p\frac{\partial T}{\partial t} - L\rho_i\frac{\partial \theta_i}{\partial T}\frac{\partial T}{\partial t} + \nabla\cdot\left(\boldsymbol{q}^{T_{cnd}} + \boldsymbol{q}^{T_{adv}}\right) = r^{T_0} \tag{29}$$

Recalling Eqs. 26 and 27, Eq. 29 can take the form of

$$C_T\frac{\partial T}{\partial t} + \nabla\cdot\left(-\lambda_T\nabla T + \rho_w c_w T\left(-\frac{\boldsymbol{K}^{S_w}}{\rho_w g}\nabla(\Psi + \rho_w \boldsymbol{g} z)\right)\right) = r^{T_0} \tag{30}$$

where $C_T = C_p + L\rho_i\phi\partial S_w/\partial T$ is the apparent volumetric heat capacity.

Validation and Demonstration

The THM formulation and the TEVP constitutive model have been numerically implemented into the finite element software DISROC developed by Fracsima [3]. This implementation enables parallel operation with the DISROC solver, the graphical user interface, and the pre- and post-processor GID, providing a setup for analyzing time and temperature-dependent behavior of frozen soils. This section evaluates the numerical predictions of thermal creep deformations in frozen samples under a triaxial creep setup by comparing them with experimental results. The capabilities of the THM framework are then demonstrated through a one-dimensional freezing problem, showcasing its effectiveness in capturing key features of freezing processes in soils.

Thermal Creep Deformations Under Triaxial Testing

Numerical simulations are conducted to replicate the triaxial creep tests performed by Wang et al. [4] on frozen clay samples, highlighting the accuracy of the implemented constitutive model. The simulations focus on capturing the development of thermo-viscoplastic strains under varying deviatoric and confining stress conditions, modeled at two specific temperatures: -0.5 °C and -1.5 °C. The model parameters governing the material behavior are detailed in Table 1.

Table 1: Model parameters used in the simulation of triaxial creep tests.

$G_0\,(MPa)$	$E_{ref}\,(MPa)$	$a_E\,(K^{-1})$	$\kappa_o\,(-)$	$\lambda_o\,(-)$	$N_o\,(-)$	$p_o^*\,(MPa)$
3	100	0.1	0.01	0.02	1.62	0.28
$p_r^*\,(MPa)$	$M\,(-)$	$\nu_f\,(-)$	$a_\lambda\,(-)$	$b_\lambda\,(MPa^{-1})$	$p_{t_b}^*\,(MPa)$	$a_s\,(MPa^{-1})$
0.05	0.95	0.48	0.49	0.15	3	0.12
$\kappa_s\,(-)$	$\psi_o\,(-)$	$a_\psi\,(K^{-1})$	$t_{f_o}\,(min)$	$p_{co}^*\,(MPa)$	$a_\sigma\,(K^{-1})$	$a_t\,(-)$
0.008	0.022	0.1	167	1	0.5	1
$t_o\,(min)$	$Z\,(-)$					
2	1					

Figure 1 illustrates a comparison between the numerical results and experimental measurements. The figure illustrates the strong agreement between the two, demonstrating the reliability of the numerical model. The framework effectively captures notable changes in the magnitude and evolution of deviatoric creep strains as deviatoric stress increases. Such stress-dependent behavior is more evident at temperatures near 0 °C, reflecting the transition of soil creep into the tertiary stage. These results highlight the effectiveness of the numerical formulation in simulating the complex thermal creep response of frozen soils subjected to various triaxial loading conditions.

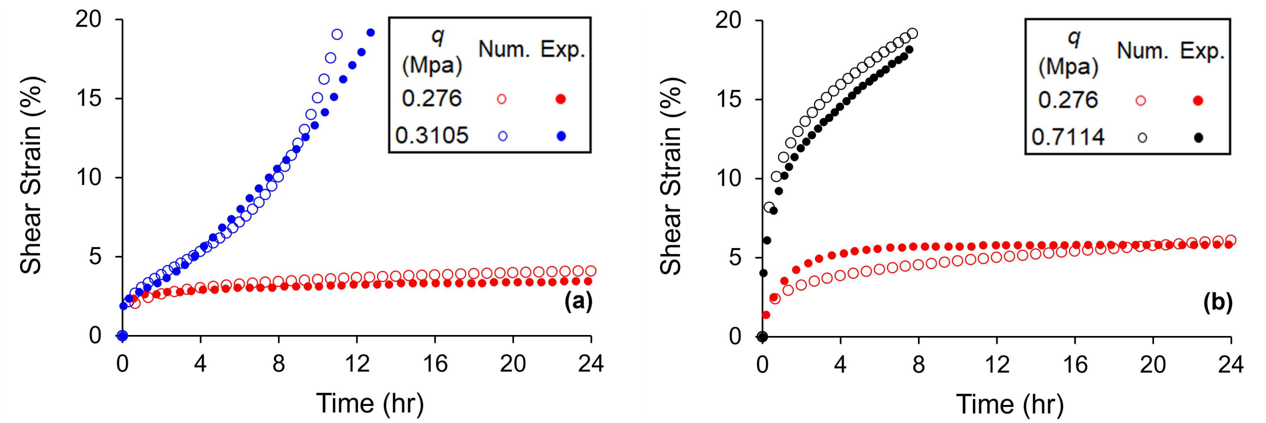

Figure 1: Comparison of experimental and numerical responses of a frozen clay sample under triaxial creep test: shear strain-time plot at (a) T = -0.5 °C and σ_{33} = 1.2 MPa; and (b) T = -1.5 °C and σ_{33} = 0.3 MPa.

Numerical Simulation of One-Dimensional Freezing Problem

This section focuses on a thermo-hydro-mechanical (THM) simulation, investigating the reciprocal effects of heat transfer, water movement, and mechanical responses in a one-dimensional soil freezing problem. A plane strain model with dimensions of 1 m × 0.2 m representing a fully saturated soil sample subjected to an initial uniform temperature of 2 °C is considered (see Figure 2). A convection-type heat flux of $q = 50(T - T_\infty)$ is applied to the top boundary, while the bottom boundary is held at a constant temperature of 2 °C to initiate freezing at the top surface advancing downward along the vertical axis. The lateral boundaries are thermally insulated. Hydraulic flux is permitted only through the bottom boundary; all other surfaces assumed impermeable. The bottom boundary of the model is mechanically restricted and horizontal displacements are restricted on the lateral boundaries. The material parameters used for this analysis are detailed in Table 2. This simulation aimed to demonstrate the model's ability to capture freezing-induced processes rather than replicate a specific soil response. Accordingly, thermal and hydraulic parameters were adopted from well-established literature values, while the mechanical parameters for the TEVP model were taken from a previously calibrated and validated dataset [2].

Table 2: Material parameters used in the soil freezing THM simulation.

$G_0\,(MPa)$	$E_{ref}\,(MPa)$	$a_E\,(K^{-1})$	$\kappa_o\,(-)$	$\lambda_o\,(-)$	$N_o\,(-)$	$p_o^*\,(MPa)$
5	180	0.1	0.1	0.2	3.75	0.28
$p_r^*\,(MPa)$	$M\,(-)$	$\nu_f\,(-)$	$a_\lambda\,(-)$	$b_\lambda\,(MPa^{-1})$	$p_{t_b}^*\,(MPa)$	$a_s\,(MPa^{-1})$
0.05	1.1	0.3	0.49	0.15	12	0.053
$\kappa_s\,(-)$	$\psi_o\,(-)$	$a_\psi\,(K^{-1})$	$t_{f_o}\,(min)$	$p_{co}^*\,(MPa)$	$a_\sigma\,(K^{-1})$	$a_t\,(-)$
0.008	0.014	0.006	167	0.33	0.093	7.8
$t_o\,(min)$	$Z\,(-)$	$\phi_0\,(-)$	$K\,(m/s)$	$b\,(-)$	$Mb\,(kPa)$	$m\,(-)$
30	1	0.34	5.59×10^{-6}	1	6857142.9	0.7
λ_s $(W/m/K)$	λ_w $(W/m/K)$	λ_i $(W/m/K)$	C_s $(J/m^3/K)$	C_w $(J/m^3/K)$	C_i $(J/m^3/K)$	μ $(-)$
1.8	0.56	2.23	2385000	4180000	1925700	0.004

To capture the effects of cryogenic suction and temperature-induced water migration during freezing, the simulation illustrates the redistribution of unfrozen water driven by phase transitions and thermal gradients. Figure 2 presents these cryo-driven processes, highlighting both the movement of water and the associated development of frost heave after 10 days. As shown in Figure 2a and b, the temperature distribution changes across the sample over time in response to the applied (negative) heat flux; it is accompanied by a rapid decrease in unfrozen water saturation. The phase transition of water to ice induces volumetric expansion, resulting in a substantial migration of unfrozen water towards the adjacent unfrozen zone. In contrast, under freezing conditions, the remaining unfrozen water may also migrate towards the already frozen region, further amplifying the progression of the freezing front. This interplay between downward expulsion and upward cryo-pumping of unfrozen water governs the location of the maximum porosity increase (see Figure 2c). The development of frost heave is illustrated in Figure 2d.

Conclusions

This study presents a new thermo-hydro-mechanical (THM) formulation to investigate the complex time- and temperature-dependent behavior of frozen soils. The proposed framework

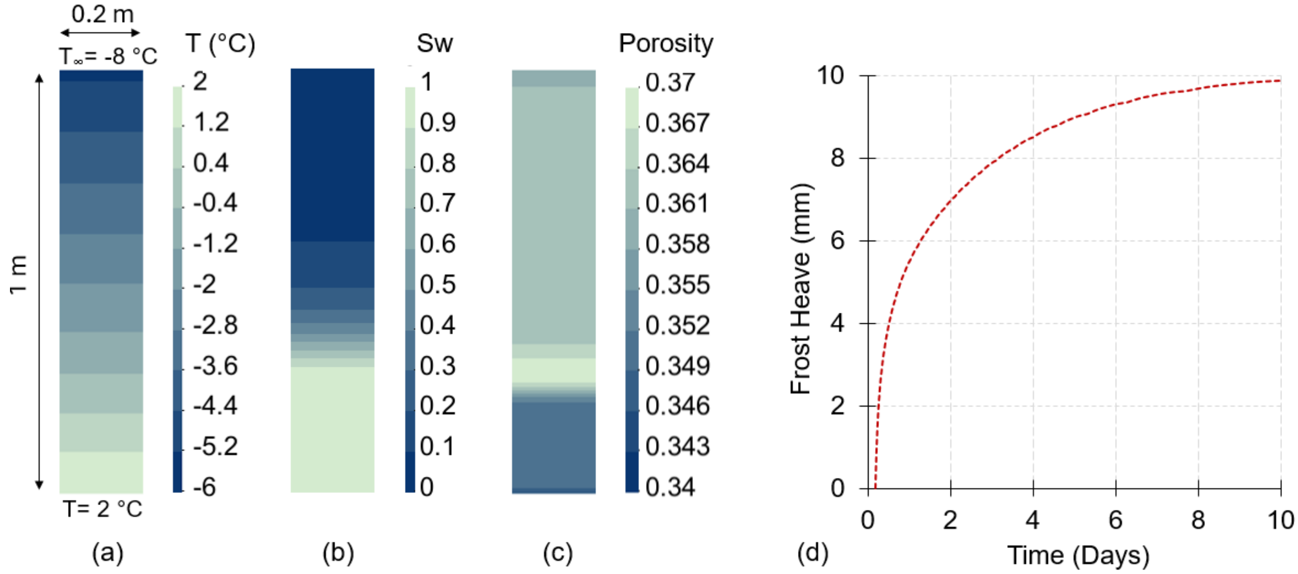

Figure 2: Variation of (a) temperature, (b) unfrozen water saturation, (c) porosity with depth after 10 days and (d) frost heave development with time.

advances conventional modeling approaches by treating the partially frozen medium as a deformable solid mixture of ice and soil grains, with a porous space filled with unfrozen water. The inclusion of an advanced strain-rate constitutive model enables the simulation of thermal creep deformations, while the hydraulic and thermal governing equations comprehensively account for the reciprocal interactions of unfrozen water and ice, as well as latent heat effects during phase transitions. Numerical simulations highlight the capability of the THM framework in capturing key phenomena, such as water migration, porosity evolution, and frost heave, offering a reliable framework for predicting the long-term response of frozen foundations.

References

[1] Olivier Coussy. *Poromechanics*. John Wiley & Sons, 2004.

[2] Dana Amini, Pooneh Maghoul, Hartmut Holländer, and Jean-Pascal Bilodeau. A critical state-based thermo-elasto-viscoplastic constitutive model for thermal creep deformation of frozen soils. *Acta Geotechnica*, pages 1–19, 2023.

[3] Fracsima. DISROC, a finite element code for modeling thermo-hydro-mechanical processes in fractured porous media, 2016.

[4] Pan Wang, Enlong Liu, Bin Zhi, Bingtang Song, and Jian Kang. Creep characteristics and unified macro–meso creep model for saturated frozen soil under constant/variable temperature conditions. *Acta Geotechnica*, pages 1–21, 2022.